

GdN nanoislands as midgap states for low resistance GaN tunnel junctions

Sriram Krishnamoorthy^{†}, Thomas F. Kent[‡], Jing Yang[‡], Pil Sung Park[‡], Roberto C. Myers^{‡,†}, Siddharth Rajan^{†‡*}*

[†]Department of Electrical and Computer Engineering and [‡]Department of Materials Science and Engineering, The Ohio State University, Columbus, OH 43210, United States

KEYWORDS

Midgap states, tunnel junctions, Nanoislands, GaN, GdN , molecular beam epitaxy, light-emitting diode.

ABSTRACT

We show that GdN nanoislands can enhance inter-band tunneling in GaN PN junctions by several orders of magnitude, enabling low optical absorption low-resistance tunnel junctions (specific resistivity $1.3 \times 10^{-3} \Omega\text{-cm}^2$) for various optoelectronic applications. We exploit the ability to overgrow high quality GaN over GdN nanoislands to create new nanoscale heterostructure designs that are not feasible in planar epitaxy. GdN nanoisland assisted inter-band tunneling was found to enhance tunneling in both of the polar orientations of GaN. Tunnel injection of holes was confirmed by low temperature operation of GaN p-n junction with a tunneling contact layer, showing strong electroluminescence down to 20K. The availability of

tunnel junctions with negligible absorption could not only improve the efficiency of existing optoelectronic devices significantly, but also enable new electronic and optical devices based on wide band gap materials.

TEXT

Interband tunnel junctions could improve the efficiency and functionality of a variety of III-nitride semiconductor devices for visible and ultra violet emitter and photovoltaic applications.¹⁻⁷ The low ionization efficiency of p-type dopants and low hole mobility lead to high parasitic resistances in III-nitride optoelectronics that cause significant losses in devices such as energy-efficient solid state lighting LEDs, laser diodes. N-type tunneling contacts to resistive p-type layers could lead to significant improvement in the efficiency of light emitting diodes (LED), lasers, and solar cells. Tunnel junctions are an essential component for device structures such as multi- junction solar cells and multiple active region LEDs. In particular, efficiency improvements in LEDs for energy efficient solid state lighting can have global energy impact.

However, in wide band gap materials such as GaN, it is extremely challenging to achieve interband tunneling between p-type and n-type regions. The larger band gaps in this system and dopant solubility limitations lead to thicker depletion regions, large energy barriers to tunneling and higher tunneling resistance than in lower gap semiconductors, and traditional heavily doped p-n junctions⁸ can therefore not provide low tunneling resistance. Recently, the spontaneous and piezoelectric polarization^{9,10} in the III-nitride system using structures like GaN/AlN/GaN,³⁻⁵ GaN/InGaN/GaN,¹¹⁻¹³ and AlGaIn/GaN¹⁴ were used to overcome limitations imposed by the large energy band gap. While GaN/InGaN/GaN tunnel junctions with very low resistance have been

demonstrated,⁶ the dependence on crystal polarity and the high absorption coefficient of InGaN limit the application of this approach in devices.

Mid-gap states created by intentional defects can be used to overcome tunneling resistance limitations imposed by constraints such as the energy gap and dopant solubility by providing intermediate states that can reduce the tunneling width between p and n regions in a tunnel diode, as shown in Figure 1a. In the GaAs system, this idea was successfully used to improve tunneling using low temperature (LT) molecular beam epitaxy (MBE) grown GaAs¹⁵, where native point defects provided the mid-gap states, and epitaxial semi metallic ErAs¹⁶⁻¹⁸ and MnAs¹⁹ nanoparticles in GaAs, where the nanoscale islands provide intermediate states to assist in tunneling. In this paper, we show for the first time that rare earth nitride (GdN) nanoislands can create mid-gap states in a PN junction that enhance interband tunneling by *several orders of magnitude*.

Bulk GdN^{20,21} is a cubic rock salt semiconductor with a theoretical indirect band gap of 0.7-0.85 eV²¹ and (111)-oriented GdN has a 9.4% lattice mismatch with the basal plane of wurtzite GaN. GdN nanoislands have successfully been demonstrated on c-plane GaN,²² additionally, it was shown that high quality single crystalline GaN layers with could be overgrown on these nanoislands²² without nucleating any new extended defects in the overlayer. The formation of GdN as nanoparticles is important because, GaN overgrown on planar (111) GdN²³ was found to be polycrystalline due to broken rotational symmetry along the c-axis. The ability to grow high quality crystalline GaN on top of GdN enables us to embed nanoislands within a matrix of single crystal GaN, while maintaining high crystalline quality in the GaN. Such *nanoheterostructures* extend the functionality of III-nitrides by enabling energy band profiles and mid-gap states that would not be achievable within the (In,Ga,Al)N alloy system.

Furthermore, the indirect gap of GdN leads to negligible absorption at visible wavelengths (see supporting information), which is a critical criterion for incorporation into optoelectronic devices. GdN nanoislands therefore provide a promising way to create mid-gap state-enhanced tunnel junctions in the III-nitride system.

GaN p^+ -GaN/GdN nanoisland/ n^+ -GaN junctions as depicted in Figure 1b were grown along N-face (000-1) and Ga-face (0001) orientations using N_2 plasma-assisted molecular beam epitaxy (PAMBE). GdN coverage was incomplete and deposition of 2.4 ML of GdN resulted in a partial coverage with 3 nm tall islands oriented along the [111] direction on wurtzite [0001] GaN.²² Details about island formation dynamics and transmission electron microscope images of the islands are described elsewhere.²² A 50 nm p-type GaN was grown on top of the GdN nanoislands, and was found to be single crystalline based on in-situ reflection high-energy electron diffraction, as expected from previous work.²² The structure was capped with a 30 nm heavily p-type doped GaN layer to enable formation of low resistance ohmic contacts. The device was processed using contact lithography, with Ti (20nm)/Au (200nm) ohmic contact for the GaN:Si layer and Ni(20nm)/Au(200nm) ohmic contact on p^{++} GaN cap. Additional details of the growth conditions used in this work is presented in the supporting information.

The principle of GaN/GdN/GaN tunnel junction operation is explained here. Under forward bias, the holes in the valence band of p-GaN and electrons in the conduction band of n-GaN tunnel into states in GdN and recombine. Since the forward bias current does not rely on direct band to band tunneling (from n-GaN to p-GaN), we do not expect band-crossing related negative differential resistance (as expected in a normal heterojunction Esaki diodes). In reverse bias, electrons in the valence band of p-GaN tunnel into conduction band of n-GaN via states in GdN.

The temperature dependent electrical characteristics of the Ga-polar GaN/GdN/GaN TJ (20 μm X 20 μm) are shown in Figure 1c. At a reverse bias of 1 V, the current density changes from 7.8 A/cm² at 77 K to 78 A/cm² at 300K. The weak temperature dependence shows that the dominant transport mechanism is tunneling. The IV curves in the low temperature, high current regime had a quadratic dependence, indicating that space charge limited transport may be playing a role.²⁴ This shows that after hole freeze out (which occurs at relatively high temperatures due to the high ionization energy of Mg), holes are injected through the tunnel junction and travel across the p-doped region. Further details are in the Supporting information. Figure 2a shows the room temperature electrical characteristics of the Ga-polar and N-polar TJ devices. At a reverse bias of 1 V, the Ga-polar GaN/GdN/GaN device had a current density 78 A/cm², while the same epitaxial layer grown along the N-polar orientation had a comparable current density of 99 A/cm². This indicates that GaN/GdN/GaN tunnel junctions have relatively weak dependence on crystal orientation and polarization in the reverse direction. However, in the forward bias, as shown in Figure 2a, the N-polar TJ shows higher current density than the Ga-polar TJ. This is because the polarization field in GdN is in the same direction as the depletion field in case of N-polar TJ. This effect is in fact quite similar to reduced turn-on voltage reported in previous work on N-polar green LEDs.²⁵

The relatively weak dependence of the tunneling current on crystal orientation and polarization in the reverse direction can be understood from the band diagram of the structures. To calculate the energy band diagram of a p-GaN/3 nm GdN/n-GaN heterojunction, we model GdN as a non-polar material with a narrow bandgap²¹, and assume that the polarization discontinuity at the GaN/GdN interface leads to an interface charge density that is equal to the spontaneous polarization sheet charge of GaN. This is depicted in the charge diagram in Figure

2b, for the Ga-face and N-face oriented PN junctions. For p-GaN up structure, the field due to the spontaneous polarization sheet charge dipole $\sigma_{sp,GaN}$ is in the same direction as that of the depletion field in case of N- polar, where as the direction is opposite in the case of Ga – polar structure. The effect of doping in GaN on the band diagram is simulated using a self consistent Schrödinger Poisson solver²⁶, and is shown in Figure 2c,d, for Ga-polar and N-polar case respectively, assuming equal conduction band offset and valence band offset and a dielectric permittivity²¹ of 7. The depletion width is expected to be lower in the N-polar case than in the Ga-polar case, with the difference being less significant as the doping density is increased. At the highest doping density shown ($N_D = N_A = 5 \times 10^{19} \text{ cm}^{-3}$), the depletion field exceeds the polarization field and the band diagram looks similar for both the orientations, and the depletion width is not significantly different in the two cases.

To confirm tunneling injection of holes, we designed n-GaN/GdN/p-GaN/n- GaN structure (sample A) as shown in Figure 3a. The hole concentration in the p-GaN layer ($[Mg] = 1 \times 10^{18} \text{ cm}^{-3}$) is expected to be $1.1 \times 10^{17} \text{ cm}^{-3}$. This structure uses an n-GaN/GdN/p-GaN tunnel junction to contact the p-GaN layer of a GaN PN junction, thereby eliminating the need for a metal p-contact. As the PN junction is forward biased, the GaN/GdN tunnel junction is reverse biased. Electrons from the valence band of p- GaN tunnel into n-GaN, leaving a hole behind in the p-GaN layer. This is equivalent to tunnel injection of holes from an n-GaN contact into the p-type material, and so if the tunnel junction is ideal, we expect this structure to behave like a simple PN junction. The two important requirements for such a tunnel junction to be incorporated in a LED or solar cell would be that (1) the voltage drop across the tunnel junction during the device operation is negligible, with appreciable tunneling close to zero bias, and (2) the specific resistivity of the tunnel junction is minimal. The structure with the GaN/GdN TJ

contact layer was compared with a structure with a reference p⁺-n⁺ GaN TJ contact layer (sample B) that has the same structure as sample A, but without the GdN nano island layer.

Growth and fabrication procedures described earlier in this Letter were used to obtain the device shown in Figure 3a. Atomic force microscope image (Figure 3b) of the sample surface shows typical step flow growth morphology with a low rms roughness of 0.6 nm. As expected, the electrical characteristics of the device shown in Figure 3c were similar to that of a GaN PN junction. The forward turn on voltage of this device with the incorporation of a tunnel junction is the sum of the voltage drop across the forward biased p n junction and the voltage drop across the reverse biased tunnel junction. At a reference current density of 20 A/cm², the p contact-less PN junction with GaN/GdN TJ (Sample A) had a voltage drop of 3.05 V, compared to 4.5 V for the p⁺-n⁺ GaN TJ device(Sample B) . This indicates an additional voltage drop of 1.45 V across the p⁺-n⁺ GaN TJ, which is similar to past reports where a GaN based tunnel junction LEDs led to an extra voltage drop ranging from 0.6 V to 1.5 V^{1,2}. To estimate the voltage drop, the resistance of the device with GaN/GdN TJ (Sample A) in forward bias was calculated from a fit of the linear portion of the forward bias characteristics, to be 1.3 X 10⁻³ Ω-cm². This includes the contact resistance, series resistance in the p-GaN and n-GaN regions, and the tunnel junction resistance. The top contact resistance was measured using transfer length method (TLM) method, and found to be 1.3 X 10⁻⁵ Ω-cm². The estimated series resistance of the thin p-GaN (~10⁻⁵ -10⁻⁶ Ω-cm²) and n-GaN layers (~10⁻⁷ Ω-cm²) used in this study are negligible compared to the measured total forward bias resistance. Hence, the specific tunnel junction resistivity can be extracted to be 1.3 X 10⁻³ Ω-cm². At a reference current density of 20 A/cm² the voltage drop across the GaN/GdN TJ would be 64 mV, which is negligible compared to the turn-on voltage of the GaN PN junction.

The temperature dependent electrical characteristics of sample A is shown in Figure 3d. Even at 77 K, where freeze out of holes is expected, a high current density is observed in forward bias. A current density of 20 A/cm² is observed at 3.55 V forward bias at 77 K, compared to 3.05 V at room temperature. At 6 V bias, the current drops from 1.4 kA/cm² at 300 K to 266 A/cm² at 77 K (a factor of 5 lower), indicating efficient injection of holes at low temperature, with tunneling being the dominant mechanism. In addition, the device is observed to give bright blue-UV electroluminescence at both low temperature and room temperature, as shown in Figure 3e. At 20K, the band to band (3.4eV), and band to acceptor (3.2eV) emission in GaN is observed with two additional peaks marked as peak A and peak B. The origin of these peaks could be related to defect levels in GaN, or emission from GdN, or absorption of UV photons in GdN and reemission. Nevertheless, the strong electroluminescence signal obtained at low temperature, indicates efficient hole injection due to the tunnel junction. Excellent current spreading resulting in a uniform light emission was observed (inset of Figure 3e) even with minimal contact metal coverage, thereby minimizing the absorption loss due to the contact metal and enhancing light extraction.

To benchmark these results against the literature, the lowest specific tunnel junction resistivity achieved in different material systems are compared in Figure 3f.^{3,5,27-29} It is evident from the figure that tunnel resistivity increases exponentially with band gap, and that while low resistivity in wider band gap materials such as GaN is an inherent challenge, heterostructure engineering using GdN nanoparticles provides a route to overcome this limitation. The low tunnel resistivity achieved in this work would lead to negligible tunnel junction voltage drop loss for the typical drive current in LEDs and solar cells. Further investigations are necessary to understand the true band line-up, interfacial dipoles, and related effects in these heterostructures.

Optimization of the island size, density, and growth conditions could help to reduce the resistance further, which would enable incorporation in high brightness LEDs.

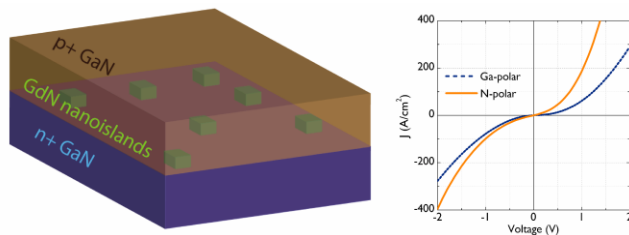
With the availability of tunnel junctions for both Ga-polar and N-polar oriented layers, several promising applications and directions for GaN electronics and optoelectronics can now be imagined. Several groups have indicated the advantages of N-polar P-up^{25,30,31} or Ga-polar P-down^{32,33} LEDs. However, P-down LEDs have been limited due to the large p-type layer spreading resistance, and therefore need a tunnel junction to connect the p-layer to an n-type substrate. Heterostructure polarization engineering based approaches using InGaN are not effective since they work for N-polar oriented P-down PN tunnel junctions⁶ and not for a Ga-polar oriented P-down PN junctions. The alternate approach (using GaN/AlN/GaN) could be used for the aforementioned cases, but does not provide low enough tunneling resistance to be useful. The GdN approach presented here overcomes these limitations by enabling both Ga-polar and N-polar oriented PN junctions. GdN nanoislands could also be embedded in wide band gap barriers, combining polarization and nanoparticle engineering for lower resistance. Previous work on GaN TJ LED^{1,2,34} showed an improved current spreading leading to enhanced light output. However the TJ LED devices had an additional voltage drop across the TJ. The efficient low resistance tunnel junction achieved in this work can be incorporated to enhance the performance of top emitting LEDs. Another interesting application is the incorporation of low resistance tunnel junctions in vertical cavity emitters³⁵ where current spreading and resistance of p-type layers are major issues. The magnetic properties of GdN²⁰ and high tunneling current density could also enable spintronic devices that benefit from the high spin lifetimes in GaN.³⁶ The design of GaN bipolar devices such as PN diodes and BJTs has been limited by p-type contacts and resistance. Low resistance tunnel junctions can now be used to re-design these

bipolar devices to achieve greater performance or functionality. Finally, since GdN-based junctions do not require polarization, they could also be used to improve performance for emerging non-polar and semi-polar GaN devices.

In summary, we demonstrated that epitaxial GdN nanoislands can be used for efficient inter-band tunneling in GaN PN junctions on Ga- and N-polar orientations. Efficient tunnel injection of holes from n-type GaN top contact into p-type material was achieved, and the tunnel junction specific contact resistivity of GdN was estimated to be $1.3 \times 10^{-3} \Omega\text{-cm}^2$. This demonstration of efficient tunneling using GdN nanoislands, together with previously reported polarization-engineered tunnel junctions³⁻⁵ could lead to designs for III-nitride electronic and optoelectronic devices with higher performance and functionality.

FIGURES

Table of Contents Figure



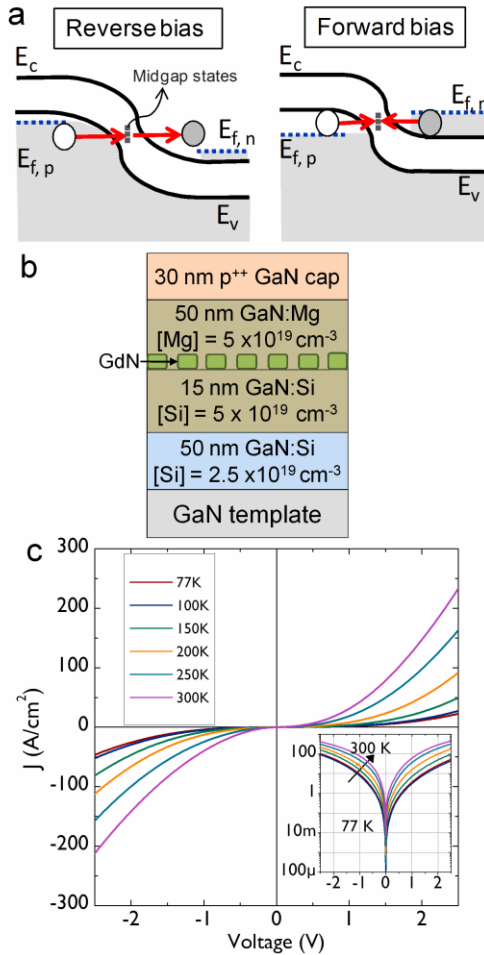


Figure 1. (a) Schematic showing operation of a mid gap states assisted tunnel junction in forward bias (electron hole recombination at mid gap states) and reverse bias(two step tunneling process through the mid gap states). (b) Epitaxial stack of GaN/GdN/GaN inter-band tunnel junction. The concentration mentioned in the figure refers to the doping density. (c) Temperature dependent electrical characteristics of Ga-polar GaN/GdN/GaN TJ Inset: Temperature dependent Log I- V characteristics

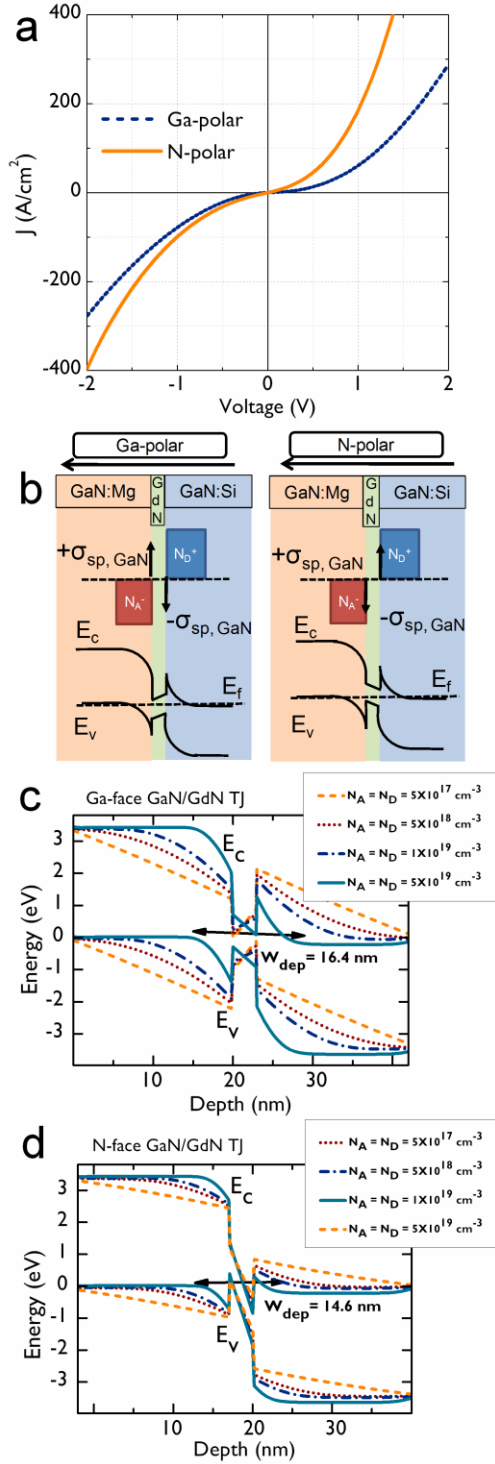


Figure 2. (a) I-V characteristics of Ga-polar and N-polar GaN/GdN/GaN TJ. Reverse characteristics of the Ga-polar and N-polar TJ shows similar current density indicating a weak polarization dependence on tunneling resistance. (b) Equilibrium charge profile and band diagram of Ga-polar, N-polar oriented p-GaN/ GdN/ n-GaN TJ. Polarization and depletion fields

are aligned for the N-polar orientation case. (c) Effect of increased doping in the case of Ga-polar and (d) N-polar p- GaN/ GdN/ n- GaN TJ.

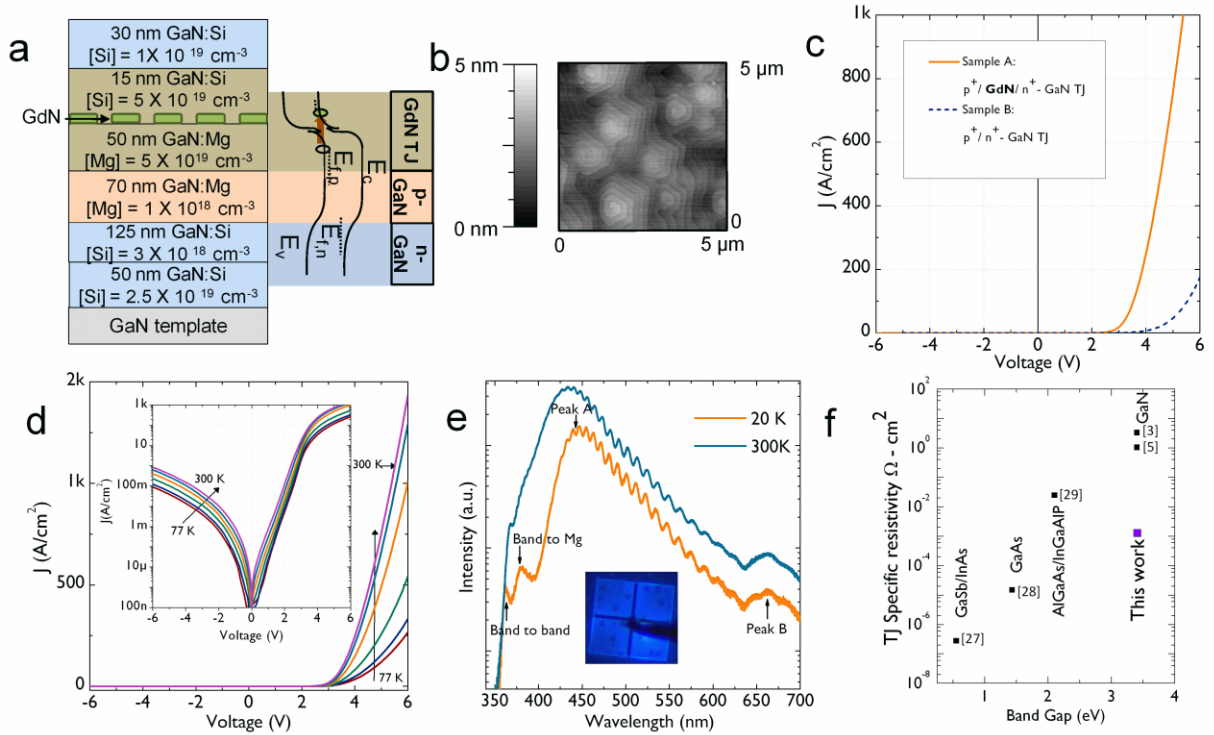


Figure 3. (a) Epitaxial stack of the p-contactless PN junction where a GaN/GdN TJ connects the p-region with the n-region. The energy band diagram shows tunnel injection of holes into p-type material from the n-type contact when the PN junction is forward biased. (b) Atomic force microscope image showing smooth surface morphology (rms roughness = 0.6 nm) (c) I- V characteristics of the p-contactless PN junction with and without GaN/GdN TJ. The sample with GaN/GdN TJ (Sample A) has negligible voltage drop across the tunnel junction, while the reference sample (Sample B) has a significant resistive drop. (d) Temperature dependent electrical characteristics of Sample A. Inset: Temperature dependent Log J- V characteristics of sample A, indicating high forward bias current even at low temperature. (e) Electroluminescence spectra obtained from sample A at 20K and room temperature. The low temperature EL shows GaN band to band as well as band to acceptor emission peaks. The additional peaks observed are marked as peak A and peak B. Inset: Optical micrograph picture of the device showing uniform blue emission. (f) Plot of specific tunnel junction resistivity achieved in different material systems as a function of band gap. The work presented here represents very low tunneling resistance achieved in GaN

ASSOCIATED CONTENT

Supporting Information. Discussion of materials and methods, space charge limited transport in GaN/GdN/GaN tunnel junctions, and absorption due to GdN nanoislands. This material is available free of charge via the Internet at <http://pubs.acs.org>.

AUTHOR INFORMATION

Corresponding Author

* Email: rajan@ece.osu.edu, krishnamoorthy.13@buckeyemail.osu.edu.

ACKNOWLEDGMENT

The authors would like to acknowledge Anup Sasikumar, Prof. Emre Gur and Prof. Steven A Ringel for low temperature measurements shown in this work. We acknowledge funding from ONR DATE MURI program (Program manager: Dr. Paul Maki).

REFERENCES

- (Word Style “TF_References_Section”). (1) Jeon, S.-R.; Song, Y.-H.; Jang, H.-J.; Yang, G. M.; Hwang, S. W.; Son, S. J. Lateral Current Spreading in GaN-based Light-emitting Diodes Utilizing Tunnel Contact Junctions. *Applied Physics Letters* **2001**, *78*, 3265–3267.
- (2) Takeuchi, T.; Hasnain, G.; Corzine, S.; Hueschen, M.; Jr, R. P. S.; Kocot, C.; Blomqvist, M.; Chang, Y.; Lefforge, D.; Krames, M. R. *et al.* GaN-Based Light Emitting Diodes with Tunnel Junctions. *Jpn. J. Appl. Phys.* **2001**, *40*, L861–L863.
- (3) Grundmann, M. Polarization-induced Tunnel Junctions in III-nitrides for Optoelectronic Applications. *Thesis (Ph.D.)University of California, Santa Barbara*, **2007**.

- (4) Grundmann, M. J.; Mishra, U. K. Multi-color Light Emitting Diode Using Polarization-induced Tunnel Junctions. *physica status solidi (c)* **2007**, *4*, 2830–2833.
- (5) Simon, J.; Zhang, Z.; Goodman, K.; Xing, H.; Kosel, T.; Fay, P.; Jena, D. Polarization-Induced Zener Tunnel Junctions in Wide-Band-Gap Heterostructures. *Phys. Rev. Lett.* **2009**, *103*, 026801.
- (6) Krishnamoorthy, S.; Akyol, F.; Park, P. S.; Rajan, S. Low Resistance GaN/InGaN/GaN Tunnel Junctions. *arXiv:1211.4905* **2012**.
- (7) Jena, D.; Simon, J.; Wang, A. (Kejia); Cao, Y.; Goodman, K.; Verma, J.; Ganguly, S.; Li, G.; Karda, K.; Protasenko, V. *et al.* Polarization-engineering in Group III-nitride Heterostructures: New Opportunities for Device Design. *physica status solidi (a)* **2011**, *208*, 1511–1516.
- (8) Esaki, L. New Phenomenon in Narrow Germanium P-n Junctions. *Phys. Rev.* **1958**, *109*, 603–604.
- (9) Bernardini, F.; Fiorentini, V.; Vanderbilt, D. Spontaneous Polarization and Piezoelectric Constants of III-V Nitrides. *Phys. Rev. B* **1997**, *56*, R10024–R10027.
- (10) Wetzell, C.; Takeuchi, T.; Amano, H.; Akasaki, I. Piezoelectric Franz–Keldysh Effect in Strained GaInN/GaN Heterostructures. *Journal of Applied Physics* **1999**, *85*, 3786–3791.
- (11) Krishnamoorthy, S.; Nath, D. N.; Akyol, F.; Park, P. S.; Esposto, M.; Rajan, S. Polarization-engineered GaN/InGaN/GaN Tunnel Diodes. *Appl. Phys. Lett.* **2010**, *97*, 203502.

- (12) Krishnamoorthy, S.; Park, P. S.; Rajan, S. Demonstration of Forward Inter-band Tunneling in GaN by Polarization Engineering. *Applied Physics Letters* **2011**, *99*, 233504–233504–3.
- (13) Growden, T. A.; Krishnamoorthy, S.; Nath, D. N.; Ramesh, A.; Rajan, S.; Berger, P. R. Methods for attaining high interband tunneling current in III-Nitrides. In *Device Research Conference (DRC), 2012 70th Annual*; 2012; pp. 163 –164.
- (14) Lee, J.-H.; Lee, J.-H. Enhanced Output Power of InGaN-Based Light-Emitting Diodes With AlGaIn/GaN Two-Dimensional Electron Gas Structure. *Electron Device Letters, IEEE* **2010**, *31*, 455 –457.
- (15) Ahmed, S.; Melloch, M. R.; Harmon, E. S.; McInturff, D. T.; Woodall, J. M. Use of Nonstoichiometry to Form GaAs Tunnel Junctions. *Applied Physics Letters* **1997**, *71*, 3667–3669.
- (16) Kadow, C.; Fleischer, S. B.; Ibbetson, J. P.; Bowers, J. E.; Gossard, A. C.; Dong, J. W.; Palmström, C. J. Self-assembled ErAs Islands in GaAs: Growth and Subpicosecond Carrier Dynamics. *Applied Physics Letters* **1999**, *75*, 3548–3550.
- (17) Pohl, P.; Renner, F. H.; Eckardt, M.; Schwanhäußer, A.; Friedrich, A.; Yüksekdag, Ö.; Malzer, S.; Döhler, G. H.; Kiesel, P.; Driscoll, D. *et al.* Enhanced Recombination Tunneling in GaAs Pn Junctions Containing low-temperature-grown-GaAs and ErAs Layers. *Applied Physics Letters* **2003**, *83*, 4035–4037.
- (18) Zide, J. M. O.; Kleiman-Shwarsstein, A.; Strandwitz, N. C.; Zimmerman, J. D.; Steenblock-Smith, T.; Gossard, A. C.; Forman, A.; Ivanovskaya, A.; Stucky, G. D. Increased

Efficiency in Multijunction Solar Cells Through the Incorporation of Semimetallic ErAs Nanoparticles into the Tunnel Junction. *Applied Physics Letters* **2006**, *88*, 162103–162103–3.

(19) Bloom, F. L.; Young, A. C.; Myers, R. C.; Brown, E. R.; Gossard, A. C.; Gwinn, E. G. Tunneling through MnAs particles at a GaAs p^+n^+ junction. *Journal of Vacuum Science & Technology B: Microelectronics and Nanometer Structures* **2006**, *24*, 1639-1643.

(20) Dhar, S.; Brandt, O.; Ramsteiner, M.; Sapega, V. F.; Ploog, K. H. Colossal Magnetic Moment of Gd in GaN. *Phys. Rev. Lett.* **2005**, *94*, 037205.

(21) Lambrecht, W. R. L. Electronic Structure and Optical Spectra of the Semimetal ScAs and of the Indirect-band-gap Semiconductors ScN and GdN. *Phys. Rev. B* **2000**, *62*, 13538–13545.

(22) Kent, T. F.; Yang, J.; Yang, L.; Mills, M. J.; Myers, R. C. Epitaxial Ferromagnetic Nanoislands of Cubic GdN in Hexagonal GaN. *Applied Physics Letters* **2012**, *100*, 152111–152111–4.

(23) Scarpulla, M. A.; Gallinat, C. S.; Mack, S.; Speck, J. S.; Gossard, A. C. GdN (1 1 1) Heteroepitaxy on GaN (0 0 0 1) by N₂ Plasma and NH₃ Molecular Beam Epitaxy. *Journal of Crystal Growth* **2009**, *311*, 1239–1244.

(24) Lampert, M. A. Simplified Theory of Space-Charge-Limited Currents in an Insulator with Traps. *Phys. Rev.* **1956**, *103*, 1648–1656.

- (25) Akyol, F.; Nath, D. N.; Krishnamoorthy, S.; Park, P. S.; Rajan, S. Suppression of Electron Overflow and Efficiency Droop in N-polar GaN Green Light Emitting Diodes. *Applied Physics Letters* **2012**, *100*, 111118–111118–4.
- (26) BandEng. Available online: <http://my.ece.ucsb.edu/mgrundmann/bandeng.htm>.
- (27) Vizbaras, K.; Törpe, M.; Arafin, S.; Amann, M.-C. Ultra-low Resistive GaSb/InAs Tunnel Junctions. *Semiconductor Science and Technology* **2011**, *26*, 075021.
- (28) Preu, S.; Malzer, S.; Döhler, G. H.; Lu, H.; Gossard, A. C.; Wang, L. J. Efficient III–V Tunneling Diodes with ErAs Recombination Centers. *Semiconductor Science and Technology* **2010**, *25*, 115004.
- (29) Sharps, P. R.; Li, N. Y.; Hills, J. S.; Hou, H. Q.; Chang, P. C.; Baca, A. AlGaAs/InGaAlP tunnel junctions for multi-junction solar cells. In *Conference Record of the Twenty-Eighth IEEE Photovoltaic Specialists Conference, 2000*; IEEE, 2000; pp. 1185–1188.
- (30) Akyol, F.; Nath, D. N.; Gür, E.; Park, P. S.; Rajan, S. N-Polar III–Nitride Green (540 Nm) Light Emitting Diode. *Jpn. J. Appl. Phys.* **2011**, *50*, 052101.
- (31) Verma, J.; Simon, J.; Protasenko, V.; Kosel, T.; Grace Xing, H.; Jena, D. N-polar III-nitride Quantum Well Light-emitting Diodes with Polarization-induced Doping. *Applied Physics Letters* **2011**, *99*, 171104–171104–3.
- (32) Reed, M. L.; Readinger, E. D.; Shen, H.; Wraback, M.; Syrkin, A.; Usikov, A.; Kovalenkov, O. V.; Dmitriev, V. A. n-InGaN/p-GaN Single Heterostructure Light Emitting Diode with P-side Down. *Applied Physics Letters* **2008**, *93*, 133505–133505–3.

(33) Newman, S.; Gallinat, C.; Wright, J.; Enck, R.; Sampath, A.; Shen, H.; Reed, M.; Wraback, M. Wavelength Stable, P-side-down Green Light Emitting Diodes Grown by Molecular Beam Epitaxy. *Journal of Vacuum Science & Technology B: Microelectronics and Nanometer Structures* **2013**, *31*, 010601.

(34) Jin An, S. Transparent Conducting ZnO Nanorods for Nanoelectrodes as a Reverse Tunnel Junction of GaN Light Emitting Diode Applications. *Applied Physics Letters* **2012**, *100*, 223115–223115–5.

(35) Diagne, M.; He, Y.; Zhou, H.; Makarona, E.; Nurmikko, A. V.; Han, J.; Waldrip, K. E.; Figiel, J. J.; Takeuchi, T.; Krames, M. Vertical Cavity Violet Light Emitting Diode Incorporating an Aluminum Gallium Nitride Distributed Bragg Mirror and a Tunnel Junction. *Applied Physics Letters* **2001**, *79*, 3720–3722.

(36) Beschoten, B.; Johnston-Halperin, E.; Young, D. K.; Poggio, M.; Grimaldi, J. E.; Keller, S.; DenBaars, S. P.; Mishra, U. K.; Hu, E. L.; Awschalom, D. D. Spin Coherence and Dephasing in GaN. *Phys. Rev. B* **2001**, *63*, 121202.

Supporting information

Materials and Methods

The samples used for this study were grown using a Veeco 930 molecular beam epitaxy(MBE) system with standard effusion cells for Ga, Si, Mg and Gd. Active nitrogen was supplied using a Veeco rf plasma source. The substrates used for this study were n-doped Ga-face GaN on Sapphire template and n-doped N-polar free standing GaN template from Saint Gobain Crystals. The substrates were cleaved into 1 X 1cm² pieces and were indium bonded on to 3 inch silicon carrier wafer. The substrates were cleaned in a ultrasonic bath with acetone, methanol and isopropyl alcohol, and baked at 400⁰ C in the buffer chamber for 1 hour, before loading into the MBE chamber. A power of 350W was applied to the nitrogen plasma unit, resulting in a growth rate of 250 nm/min for GaN, with a nitrogen beam equivalent pressure (stoichiometric flux) of 2 X 10⁻⁷ Torr. Substrate temperature was measured using an infrared pyrometer. Si and Mg doping (for Ga face and N face) was calibrated using SIMS analysis. 50 nm of 2.5E19 Si doped GaN was grown on top of the templates, using Ga rich conditions for smooth surface morphology, to serve as the bottom contact layer. The growth temperature during the growth of n+ GaN was 720⁰ C. By pulsing the N shutter, 15 nm thick highly doped n GaN (5E19 cm⁻³) was grown, after which the plasma was struck off, to remove the excess Ga from the surface. GdN was grown on a dry GaN surface using a Gd flux of 7E-9 Torr, which corresponded to a N-rich GdN growth rate of 0.4 ML/ min. Gd and N shutters were kept open for 6 mins for 2.4 ML GdN growth, which was found later to result in 3 nm tall islands.²² After 1 minute of GdN growth the RHEED pattern changed from 1 X 1 to 2 X 2 and with further growth changed back to 1X 1. The sample was cooled down to a temperature of 550⁰C for p-GaN growth. The substrate temperature during p GaN growth was lowered for the N-face stack, in order to achieve the same doping concentration as the Ga-face stack. The same growth temperatures, and beam fluxes, were used to grow the Ga-

face oriented p contact less pn junction samples with (Sample A) and without GdN nanoislands (Sample B).

Device processing steps for the p^+/n^+ tunnel junction samples is described as follows. Ni (20 nm)/ Au (200 nm) contacts were evaporated on the whole sample area using a e-beam evaporator. Optical lithography and wet etching was used to define the top contacts. The devices were isolated using ICP-RIE etching using the Cl_2 / BCl_3 etch chemistry to etch down to the n-type GaN. E-beam evaporated Ti(20 nm)/ Au(200 nm) metal stack was used to contact the n-type GaN. In case of the device processing for the p contact less PN junction samples, the only difference is the top metallization step. Optical lithography was used to define the top metal contact patterns followed by ebeam evaporation of Ti (20 nm)/ Au (200 nm) contacts and metal lift-off in acetone.

Variable temperature electrical measurements were carried out in a liquid nitrogen cooled chamber using Agilent B1500 semiconductor parameter analyzer. Electroluminescence (EL) measurements shown in this work was carried out by mounting the device in an optical cryostat with a closed cycle He cryocooler capable of temperatures from 15K-300K. EL spectra were collected using a 50mm f/2 UV grade fused silica lens with collected light subsequently focused onto the entrance slit of a Princeton Instruments SP2500i 0.5 m spectrometer and imaged with a Princeton instruments PIXIS100 UV-VIS CCD detector.

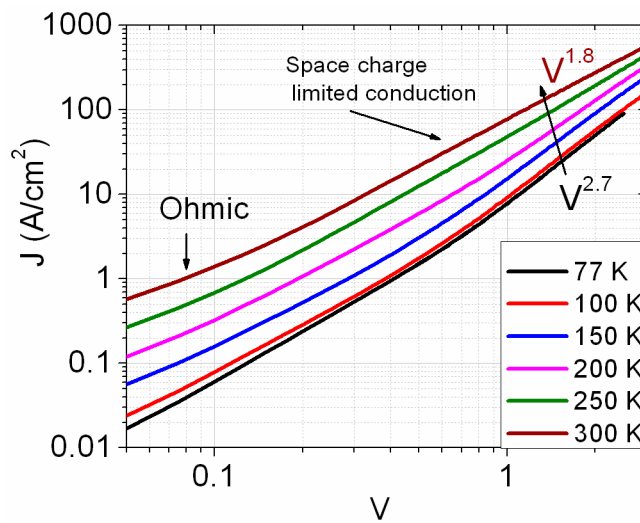
Space charge limited transport in GaN/GdN/GaN tunnel junctions

Temperature dependent electrical characteristics of Ga-face GaN/GdN/GaN TJ were shown in Figure 1c of the manuscript. The near quadratic variation of the current with voltage, as it is clear in the linear scale data presented, indicates the space charge limited conduction. It becomes more

evident, in the log J- log V for the reverse bias region shown below (Supporting Information Figure 1). At low bias and current density, the current varies linearly with applied voltage and is marked as the ohmic region in the plot. However, at high current density, the current voltage variation can be fitted with the expression

$$J = a * V^b$$

The fitting parameter b is found to vary from 2.7 to 1.8 as the temperature is increased from 77 K to 300 K. The linearity in log J- log V plot can be explained using a trap limited space charge limited conduction mechanism²⁴ which has similar power relationship as observed in the GaN/ GdN/ GaN TJ samples.

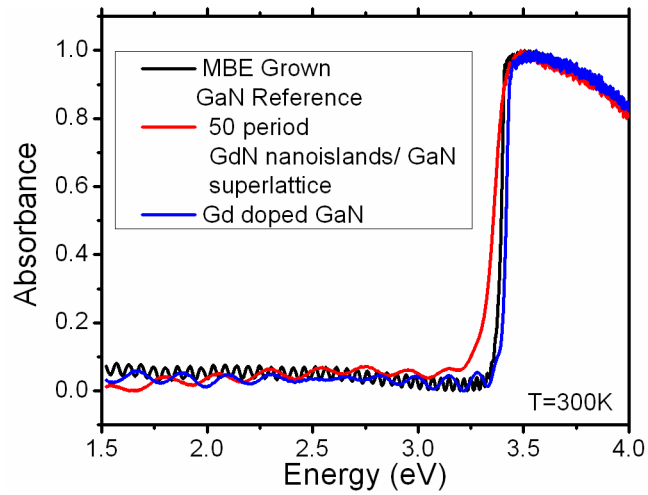


Supporting Information Figure 1. Log J- Log V characteristics of GaN/GdN/GaN TJ in reverse bias

Absorption due to GdN nanoislands

For incorporation of GdN nanoislands based tunnel junctions in visible light emitters, the absorption of visible light by GdN nanoislands must be minimal. Absorption spectra of a 50

period GdN nanoisland/ GaN super lattice stack is shown in Supplementary Information Figure 2. Absorption spectra were collected by passing a white light spectrum (300nm-2000nm) from a 350W Xe arc lamp through the samples, which have been optically polished on the sapphire side of the wafer. A reference spectra of the Xe arc lamp is collected by passing the arc lamp through the quartz window that the samples are mounted on and focusing it onto the slit of a 0.5m spectrometer equipped with a UV-VIS CCD (PI PIXIS 100) and NIR diode array (PI OMA-V 2.2um). Spectra are then collected for the samples of interest and are normalized by the reference spectra to reflect the absorbance due to the sample. All samples exhibit Fabry Perot interference fringes, indicative of high quality interfaces and measurement optical alignment. In the UV-visible region, the clear bandgap absorption feature of GaN reference sample at 3.4eV is evident. The sample with 50 period GdN nanoislands /GaN superlattice exhibits additional absorption features that persist to 3.2 eV. By comparison with the absorbance spectra from a Gd doped GaN film ($[Gd]=7E17cm^{-3}$) which does not exhibit this band, it was confirmed that the additional adsorption is likely due to the presence of the GdN nanoparticles and not due to a Gd impurity related deep level. Hence the absorption for a single period of GdN nanoisland, that has been used in this tunnel junction work, is expected to be negligible for the blue and green wavelengths. Non-absorbing low resistance tunnel junction demonstrated in this work, can hence be incorporated in commercial visible LEDs.



Supporting Information Figure 2. UV-Visible absorbance spectra for Gd containing samples and reference